Determining Size-Specific Dose Estimates for Helical Head CT Examinations Using Monte Carlo Methods

Anthony J. Hardy[1,2]; Maryam Bostani, Ph.D[1,2]; Andrew M. Hernandez, Ph.D[3]; Maria Zankl, MSc[4]; Cynthia McCullough, Ph.D[5]; Chris Cagnon, Ph.D[1,2]; John M. Boone, Ph.D[3]; Michael McNitt-Gray, Ph.D[1,2]

[1]Department of Radiology, David Geffen School of Medicine, University of California, Los Angeles, Los Angeles, California, 90024

[2]Physics and Biology in Medicine Graduate Program, David Geffen School of Medicine, University of California, Los Angeles, Los Angeles, California, 90024

[3]Departments of Radiology and Biomedical Engineering, Biomedical Engineering Graduate Group, University of California Davis, Sacramento, California 95817

[4]Helmholtz Zentrum München, German Research Center for Environmental Health (GmBH), Research Unit Medical Radiation Physics and Diagnostics, Ingolstaedter Landstrasse 1, Neuherberg 85764, Germany

[5]Department of Radiology, Mayo Clinic, Rochester, MN, 55905

***Corresponding Author**
924 Westwood Blvd, Suite 650
Los Angeles, CA 90024, USA
Phone: (310) 481-7558
ahardy@mednet.ucla.edu

Purpose

Size Specific Dose Estimates (SSDE) conversion factors have been determined by AAPM Report 204 to adjust $CTDI_{vol}$ to account for patient size but were limited to body CT exams. The purpose of this work was to determine conversion factors that could be used for an SSDE for helical, head CT examinations for patients of different sizes.

Methods

Validated Monte Carlo (MC) simulation methods were used to estimate dose to the center of the scan volume from a routine, helical head exam for a group of patient models representing a range of ages and sizes. Ten GSF/ICRP voxelized phantom models and five pediatric voxelized patient models from CT image data were used in this study. CT scans were simulated using a Siemens MDCT equivalent source model. Scan parameters were taken from the AAPM Routine Head protocols for a helical protocol and scan lengths were adapted to the anatomy of each patient model. MC simulations were performed using mesh tallies to produce voxelized dose distributions for the entire scan volume of each model. Three tally regions were investigated: (1) a small 0.6 cc volume at the center of the scan volume, (2) 0.8-1.0 cm axial slab at the center of the scan volume, and (3) the entire scan volume. Mean dose to brain parenchyma in all three regions was calculated. Mean cortical bone dose and a mass-weighted average dose consisting of brain parenchyma and cortical bone were also calculated for the entire scan volume and for the slab in the central plane. All dose measures were then normalized by $CTDI_{vol}$ for 16 cm phantom. Conversion factors were determined by calculating the relationship between normalized doses and water equivalent diameter (*Dw*). Conversion factors for brain parenchyma and mass-weighted average were then compared with AAPM Report 204 conversion factors using 16 cm CTDI phantom.

Results

Brain parenchyma dose values within the 0.6 cc volume, 0.8-1.0 cm central axial slab, and the entire scan volume, when normalized by $CTDI_{vol}$ and parameterized by *Dw*, had an exponential relationship with a coefficient of determination of 0.86, 0.84, and 0.88, respectively. There was no statistically significant difference between the conversion factors across the three tally regions based on 16 cm $CTDI_{vol}$ in AAPM Report 204 and normalized brain parenchyma doses for all three regions. Exponential relationships between $CTDI_{vol}$-normalized mean cortical bone had coefficients of determination of 0.83 and 0.87 for the central slab and for the entire scan volume, respectively. $CTDI_{vol}$-normalized mass-weighted average doses had coefficients of determination of 0.39 and 0.51 for the central slab and for the entire scan volume, respectively. A significant difference was observed between AAPM Report 204 conversion factors and normalized mass-weighted average for the central slab and entire scan volume.

Conclusions

Conversion factors that could be used for an SSDE for routine, helical head CT exams were determined for two different interpretations of center of scan volume that represent normalized dose as a function of head size using *Dw*. AAPM Report 204 conversion factors based on 16 cm CTDI phantom may serve as the basis for an SSDE for helical, head exams for normalized brain parenchyma doses for the three regions investigated in this study. AAPM Report 204 conversion factors are however not applicable when the definition of center of the scan volume includes cortical bone and therefore requires a different metric such as mass-weighted average dose.

Keywords: Size-specific dose estimate, Monte Carlo dose simulations, head CT

1. INTRODUCTION

Between the years 1993 and 2006, 67×10^6 CT procedures were performed in the United States with head procedures accounting for 28.4% of the total.[1] A recent study conducted by the University of California Dose Optimization and Standardization Endeavor summarizing CT doses across twelve University of California medical centers found that head scans comprised 16% of all adult CT examinations.[2] The same study also found that most frequent area imaged in pediatric patients was the head, accounting for 33% of the total procedures administered.[2] The fact that radiation exposure from head CTs is a large contributor to total medical radiation exposures underscores the need for accurate patient dose assessments from head CT procedures, particularly for younger patients.

The radiation dose metric commonly reported on most scanners is the volume computed tomography dose index ($CTDI_{vol}$).[3, 4] This metric, however, is a measure of dose to a reference phantom, not a measure of patient dose.[3, 4] Turner et al. showed that utilizing $CTDI_{vol}$ as normalization metric for Monte Carlo (MC) simulated organs doses from abdominal CT scans compensated both for the differences among scanner manufacturers and reduced the variation of organ doses across scanners from 31.5% down to 5.2%.[5] Subsequently, AAPM Report 204 developed the size-specific dose estimate (SSDE) quantity to adjust $CTDI_{vol}$ using a set of $CTDI_{vol}$-to-patient-dose conversion coefficients from either the 32 cm or 16 cm CTDI reference phantom to account for patient size in adult and pediatric body CT exams, respectively.[6] SSDE represents an average dose to the "center of a scan volume" as defined by AAPM Report 204.[6] Although SSDE has been shown to be a good substitute for organ dose in the context of abdominal scans,[7] the work of AAPM Report 204 was limited only to body CT examinations.

The work of McMillan et al. in 2014 sought to extend the approach developed by Turner et al. and used in AAPM Report 204 for the body, to investigate organs of interest in the head, including brain and lens of eye, for routine helical and axial acquisitions.[8] In that study, strong predictive exponential correlations were observed when MC simulated organ doses from detailed voxelized phantom were normalized by 16 cm $CTDI_{vol}$ and were parameterized by water equivalent diameter (Dw) as a metric of patient size,[9] yielding coefficients of determination (R^2) of 0.93 for whole brain dose for helical cans.[8]

While predictive correlations were determined in McMillan et al., that work focused on organ doses rather than dose to the center of the scan volume, the latter being consistent with SSDE as defined in AAPM Report 204.[6]

Therefore, the purpose of this current study is to estimate dose to the "center of the scan volume" for helical head CT exams that can be used to determine conversion factors for an SSDE for the head. This work will employ voxelized patient models along with MC simulation techniques with mesh tallies of the entire head to produce voxelized dose distributions wherein two different interpretations of "center of the scan volume" will be investigated: a small central region within the brain parenchyma and a central slab comprising both brain parenchyma and cortical bone. Additionally, the entire scan volume was also investigated. In the case of the central slab, as well for the entire scan volume, doses both to the brain parenchyma and cortical bone will also be estimated. In order to take into consideration the dose received both by brain parenchyma and cortical bone in the head, a mass weighted-average dose comprising both brain parenchyma and cortical bone was devised to account for the presence both of brain parenchyma and cortical bone within the slab tally region, as well as for the entire scan volume. Per AAPM Report 204, all doses will be normalized by 16 cm $CTDI_{vol}$ and will be parameterized in an exponential fashion with Dw.

2. MATERIALS AND METHODS

2.A Patient models

Ten voxelized phantom models from the GSF family[10] and ICRP voxelized reference male and female[11, 12] were used that have all of the radiosensitive organs identified. The eight GSF voxel-based models were created from high-resolution CT images with up to 131 organs and anatomic structures segmented and the two ICRP reference male and female voxelized models were each based off modifications of two corresponding male and female GSF models of similar external dimensions. Incorporation into MC simulations required each model be represented as a three-dimensional matrix of organ or non-anatomic material such as air and the patient table as integer identification numbers wherein each identification number was allocated a material description based on elemental compositions of tissue substitutes and their densities as defined in ICRU Report 44.[13]

Additionally, to extend this investigation into the pediatric size range, the adult models were augmented with five voxelized patient models created from the image data of pediatric patients (obtained from clinically indicated scans and whose data was anonymized and collected under IRB approval), **Figure 1**. All scans were acquired on a Siemens Sensation 64 MDCT and were performed in the supine position. To create voxelized models of each patient's anatomy from the image data, voxels within each image series were modeled as either fat, water, muscle, bone or air and were subdivided into one of seventeen density levels depending on its CT number.[14] Individual organs were not segmented for these patient models but brain parenchyma tissue was semi-automatically contoured and explicitly identified. The MCNPX model characteristics for all voxelized models used in this study are summarized in **Table I**.

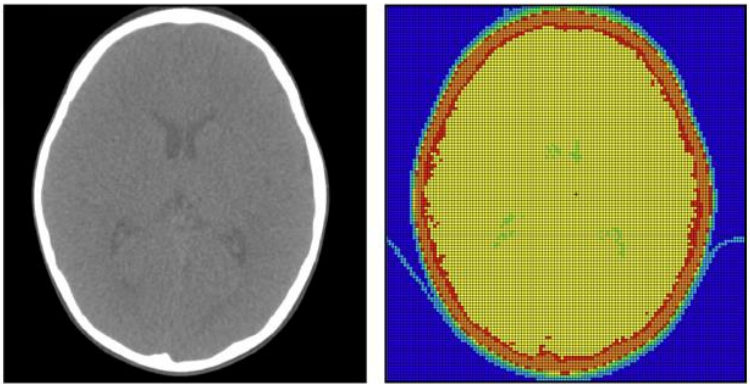

Figure 1: (Left) Head CT image of a pediatric patient who underwent a routine head exam. (Right) Monte Carlo representation of the patient wherein using a Hounsfield lookup table

Table I: MCNPX model resolution characteristics of GSF/ICRP and patient* voxelized models

Name	Gender	Age	In-plane resolution	Image slices	Column width (cm)	Row depth (cm)	Slice thickness (cm)
Peds1*	Male	7 wk	128 × 128	24	0.35	0.35	0.48
Baby	Female	8 wk	67 × 69	142	0.34	0.17	0.40
Peds2*	Male	7 d	128 × 128	30	0.35	0.35	0.48
Peds3*	Female	21 mo	128 × 128	36	0.39	0.39	0.48
Peds4*	Male	2 yr	128 × 128	30	0.35	0.35	0.48
Irene	Female	32 yr	66 × 66	348	0.75	0.38	0.50
Peds5*	Male	23 mo	128 × 128	30	0.35	0.35	0.48
Child	Female	7 yr	64 × 64	144	0.62	0.62	0.80
Helga	Female	28 yr	64 × 64	114	0.78	0.78	1.00
Golem	Male	38 yr	64 × 64	220	0.83	0.83	0.80
Donna	Female	40 yr	64 × 64	179	0.75	0.75	1.00
Frank	Male	48 yr	64 × 64	193	0.59	0.59	0.50
Visible Human	Male	38 yr	64 × 64	250	0.86	0.43	0.50
Regina	Female	38 yr	75 × 69	348	0.71	0.36	0.48
Rex	Male	43 yr	64 × 64	222	0.86	0.43	0.80

***** Indicates a voxelized patient model created from image data obtained from clinically indicated scans

2.B. CT scanner and scanning protocol

The scanning protocol used in this investigation was taken from AAPM's Adult Routine Head CT protocol.[15] All simulations were performed as fixed tube current helical scans with the voxelized models

centered within the gantry and with the patient table removed. Per the guidelines outline by AAPM for Siemens scanners and the pitch was set to 0.55. The scan range was defined from the top of the C1 lamina through the top of the calvarium.[15] The scan lengths for the GSF/ICRP phantom models[8] and the five pediatric voxelized models can be found in **Table II**. The collimation for the simulations was set to the widest nominal setting available of 28.8 mm (measure beam width of 32.2 mm) as the most dose efficient collimation for this scanner. The AAPM's Routine Head CT protocol recommend either the gantry or head be tilted to reduce the dose to the lens of the eye;[15] however, for the scanner being modeled, helical scans are not performed with gantry tilt, so no tilt angle was used in these simulations.

Table II: Scan lengths used in this investigation

Name	Scan length (cm)
Peds1	11.6
Baby	10.2
Peds2	14.3
Peds3	16.7
Peds4	14.5
Irene	15.8
Peds5	14.8
Child	14.8
Helga	14.5
Golem	15.6
Donna	16.5
Frank	21.8
Vishum	15.3
Regina	17.1
Rex	16.0

2.D Size Metrics

Water equivalent diameter (*Dw*) is an attenuation-based size metric described in AAPM Report 220 and was used in this study as a measure of patient size.[9] For the five pediatric patients, *Dw* was estimated at the center of the scan volume directly from the Hounsfield units in their image data. For the

GSF/ICRP models, it is not possible to directly calculate *Dw* since they are constructed with pixel data containing tissue identification numbers, not Hounsfield units. The *Dw* estimates for GSF/ICRP voxelized phantoms were instead obtained indirectly from a correlation between effective diameter and *Dw*.[8] **Table III** contains the head *Dw* estimates for all fifteen patients used in this investigation.

Table III: Head *Dw* estimates for the GSF/ICRP and five pediatric voxelized models from patient data

Name	Dw (cm)
Peds1	10.6
Baby	11.1
Peds2	12.6
Peds3	15.6
Peds4	15.7
Irene	17.1
Peds5	17.1
Child	17.2
Helga	18.2
Golem	18.3
Donna	18.7
Frank	19.2
Visible Human	19.6
Regina	19.9
Rex	20.2

2.D Monte Carlo simulations

All CT dose simulations for this investigation were conducting using a modified version of the radiation transport software package MCNPX (Monte Carlo N-Particle eXtended version 2.7.a).[16–18] All MC CT dosimetry for helical head scans were performed using an equivalent source model of the Siemens Sensation 64 multi-detector row CT (MDCT) scanner.[21] The equivalent source model, as previously described by Turner et al., generates and incorporates scanner-specific X-Ray spectra and bowtie filter profiles.[21]

Voxelized dose distributions of the entire head of each voxelized model were produced using the track-averaged rectangular mesh tally configuration (RMESH) within MCPNX wherein particles are tracked through a mesh grid that is independent of the regular transport problem.[16] The mesh tally grid was consistent with the resolution of each individual voxelized and was overlapped with the voxel resolution of the patient model to ensure doses on a per voxel basis were accurately estimated. The average energy deposition within each voxel were in terms of MeV/cm^3/source particle.[16] Since the mesh tally configuration is independent of the actual problem geometry, the resulting energy voxel-wise deposition maps were divided by a density map created from the conversion of tissue identification numbers from the MCNPX input files into corresponding density values to get units of MeV/g/source particle.

Normalization factors are necessary to convert dose per simulated particle (mGy/particle) to absolute dose per tube current time product (mGy/mAs). To achieve this, all MCNPX tally results were multiplied by a scanner, collimation, and beam energy specific normalization factor.[20] Each simulation was performed with 10^8 photons to ensure a relative error of less than 2% for each individual mesh element.

2.E $CTDI_{vol}$ measurements

Conventional $CTDI_{100}$ exposure measurements were taken at the center and peripheral position of a 16 cm CTDI head phantom with the scanning parameters in Sec 2.B. Exposure measurements in milliroentgen (mR) were made with a standard 100 mm pencil ionization chamber and calibrated electrometer and were thereafter converted to dose to air in mGy using the conversion factor 1 mR = 0.00876 mGy. Dose to air was then normalized by the tube current-rotation time product (mAs) used to take the initial measurements. $CTDI_{vol}$ was then calculated from the $CTDI_{100}$ measurements at the central and peripheral locations and was recorded on a dose per tube current-time product basis (mGy/mAs).

2.F Dose analyses

All dose values to all voxels in the patient models were obtained using mesh tallies as outlined in Sec 2.D. Three regions were investigated in this study: (1) a small 0.6 cc volume at the center of the scan volume, (2) 0.8-1.0 cm axial slab at the center of the scan volume, and (3) the entire scan volume. A representation of each tally region is shown in **Figure 2**. Tally regions (1) and (2) were investigated as separate interpretations representing "center of the volume." For tally region (1), a 0.6 cc volume was positioned at the center of scan volume and the mean brain parenchyma dose within this small volume were averaged and the associated standard deviation and coefficient of variations were recorded. This configuration was used to mimic a dose reading from the irradiation of 0.6 cc ion chamber virtually located in the center of head. In this last configuration, since the tally region is located in center of scan volume in the brain, only mean dose, standard deviations, and coefficients of variations for the brain parenchyma were measured. For tally region (2), dose mesh elements within a slab along an axial plane at the center of the scan volume were identified. The thickness of the slab consisted of one to two slices along the longitudinal axis of the phantom, ranging from 0.8 – 1.0 cm, depending on the slice thickness of the voxelized phantom, as detailed in Table I in Sec 2.A. The slab captures dose to the brain parenchyma, as well as dose to the cortical bone surrounding it. Under this configuration, the mean doses to both brain parenchyma and cortical bone within the slab were calculated. Standard deviation and coefficient of variation for both brain parenchyma and cortical bone within the slab were also calculated. Additionally, a mean mass-weighted average of dose contributions from both brain tissue and bone was calculated using **Equation 1**,

$$D_{wt\text{-}avg} = \frac{D_{bone}M_{bone} + D_{brain}M_{brain}}{M_{bone} + M_{brain}} \quad \textbf{(1)}$$

where D_{bone} and D_{brain} are the mean dose contributions from bone and brain parenchyma, respectively, and M_{bone} and M_{brain} represent the mass contributions from bone and brain parenchyma, respectively. Similarly, the mean doses of both brain parenchyma and cortical bone within the entire scan volume were calculated, as well as a mean mass-weighted average dose. Standard deviations and coefficients of variation for brain parenchyma and cortical bone doses within the entire scan volume were also recorded. In this study, mean doses are designated with the notion $D_{tissue,tally\ region}$ where *tissue* represents the tissue type and *tally region*

represents one of the three tally regions. The tissue contents and doses calculated within each tally region are summarized in **Table IV**.

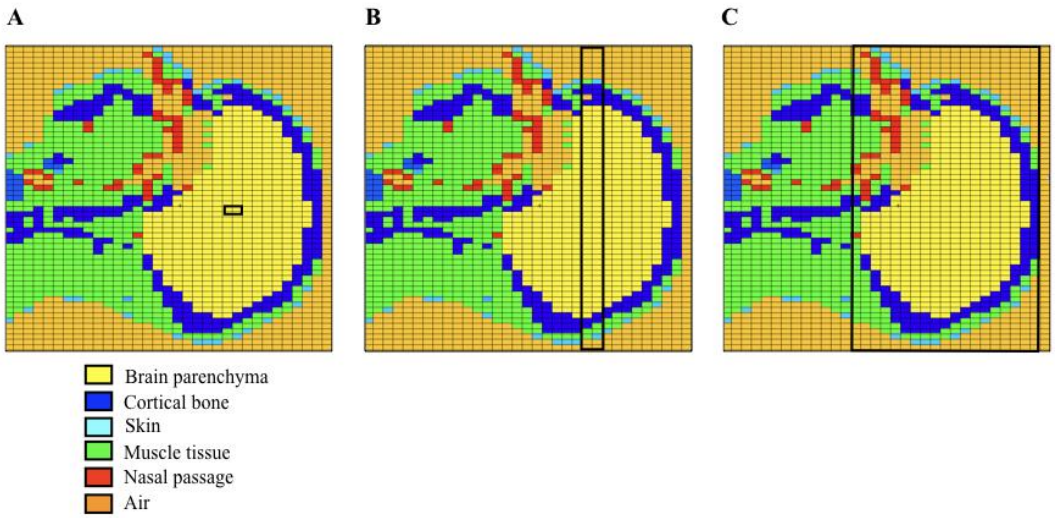

Figure 2: MCNPX voxelized representation of ICRP male "Rex" depicting **A**) the 0.6 cc volume positioned at the center of scan volume (tally region 1), **B**) the 0.8-1.0 cm axial slab positioned at the center of the scan volume (tally region 2), and **C**) the entire scan volume (tally region 3) as specified by the AAPM Routine Head CT[15] protocols with corresponding color-coded material designation for each voxel.

Table IV: Summary of tally regions, tissue contents within each tally region, and mean dose estimates measured

Tally region	Tissue(s) in tally region	Doses calculated
0.6 cc volume (1)	Brain parenchyma	$D_{brain,1}$
Central slab (2)	Brain parenchyma, cortical bone	$D_{brain,2}$, $D_{bone,2}$, $D_{wt\text{-}avg,2}$
Entire scan volume (3)	Brain parenchyma, cortical bone	$D_{brain,3}$, $D_{bone,3}$, $D_{wt\text{-}avg,3}$

All dose values were normalized by 16 cm $CTDI_{vol}$. Like AAPM Report 204, normalized dose values were parameterized as a function of Dw via an exponential relationship, as can be seen in **Equation 2**,

$$\frac{D_{tally\ region,\ tissue}}{CTDIvol} = A \times e^{-B \times Dw} \quad \textbf{(2)}$$

where *A* and *B* are regression constants for a given tissue classification. The coefficient of determination (R^2) was used to assess the ability of the correlations to explain the proportion of variation explained by Dw.

For the sake of comparison, brain parenchyma doses from all three tally regions were compared with one another using an ANOVA analysis. An ANOVA analysis was also performed to compare conversion factors from AAPM Report 204 for a 16 cm CTDI phantom with normalized brain parenchyma dose from tally regions (1), (2), and (3). Cortical bone doses for tally regions (2) and (3) were compared using a paired t-test. Similarly, mass-weighted average doses for tally regions (2) and (3) were also compared using a paired t-test. An ANOVA analysis was also performed to compare conversion factors from AAPM Report 204 with mass-weighted average doses from tally regions (2) and (3). All statistical analyses were performed using GraphPad Prism 6.00 for Mac OS X (GraphPad Software, La Jolla, California, USA, www.graphpad.com).

3. RESULTS

3.A. Mesh tally results

Three dose distribution maps from the mesh tally simulations are shown in **Figure 3**. These mesh tally results provide a graphical representation of the uniformity of the dose distribution within the brain parenchyma. Each of the following sections below describe the doses for each tissue group: brain parenchyma followed by bone dose and the mass-weighted average of brain and bone dose.

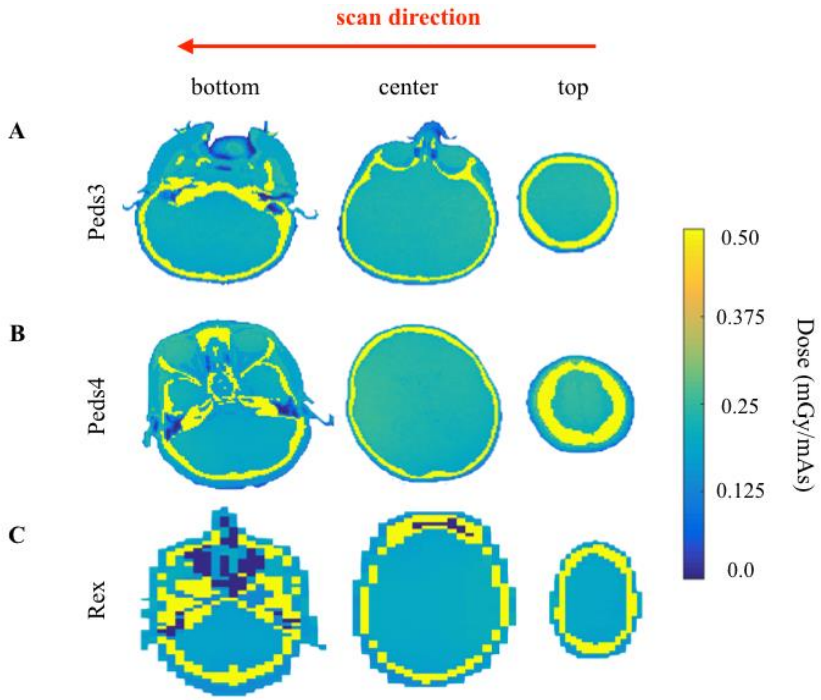

Figure 3: Axial view of voxelized dose distribution maps for Peds3 (**A**), Peds4 (**B**), and Rex (**C**), respectively, at the top, center, and bottom of the scan volume. The red arrow at the top of the figure indicates the direction of the scan range. The maps were generated by aligning rectangular mesh tallies with the resolution of MCNPX geometry. Energy deposition was tallied on a per voxel basis. Mesh tally results were then divided by the voxelized tissue density. Scanner-specific, collimation-specific normalization factors were then used to convert MCNPX dose results to units of mGy/mAs.

3.A.1 Brain parenchyma doses

In this section, the dose to the brain parenchyma for all of the different regions is reported. $D_{brain,1}$, $D_{brain,2}$, and $D_{brain,3}$, for each voxelized model can be seen in **Table V,** with ranges from 0.190 to 0.292 mGy/mAs for $D_{brain,1}$, 0.185 to 0.286 for $D_{brain,2}$, and 0.178 to 0.284 for $D_{brain,3}$. This table also shows that the coefficients of variation were below 2.6%, 6.5%, and 9.4% within tally regions (1), (2), and (3), respectively, across all voxelized models and below 3.9% across all tally regions within each voxelized model. ANOVA analysis with multiple comparison showed that $D_{brain,1}$ $D_{brain,2}$, and $D_{brain,3}$ were not significantly different from each other ($F(2, 42) = 0.07$, $P = 0.93$).

Table V: Mean brain doses by tally region type with coefficients of variation within each tally region, and the coefficient of variation across tally regions for each patient

Name	0.6 cc volume (1)		Slab (2)		Entire scan volume (3)		Across Regions
	$D_{brain,1}$ (mGy/mAs)	CV	$D_{brain,2}$ (mGy/mAs)	CV	$D_{brain,3}$ (mGy/mAs)	CV	CV
Peds1	0.290	1.7%	0.286	5.3%	0.284	4.8%	1.1%
Baby	0.292	1.4%	0.286	3.4%	0.283	5.6%	1.6%
Peds2	0.257	2.6%	0.254	4.2%	0.273	5.0%	3.9%
Peds3	0.230	2.5%	0.226	4.0%	0.238	7.3%	2.6%
Peds4	0.217	2.0%	0.215	4.8%	0.216	6.7%	0.5%
Irene	0.212	1.2%	0.210	5.6%	0.204	6.4%	2.0%
Peds5	0.200	2.6%	0.197	4.8%	0.197	5.9%	0.9%
Child	0.229	1.9%	0.227	2.9%	0.221	4.9%	1.8%
Helga	0.204	1.3%	0.207	4.8%	0.198	7.1%	2.3%
Golem	0.217	0.8%	0.211	5.0%	0.208	5.9%	2.2%
Donna	0.210	2.8%	0.214	4.4%	0.203	7.1%	2.7%
Frank	0.190	1.4%	0.185	5.0%	0.178	9.2%	3.3%
Visible Human	0.188	1.7%	0.187	6.5%	0.180	9.4%	2.4%
Regina	0.216	2.5%	0.215	5.3%	0.207	7.8%	2.3%
Rex	0.197	0.8%	0.195	3.9%	0.189	5.9%	2.1%

3.A.2 Cortical bone doses

$D_{bone,2}$ and $D_{bone,3}$, for each voxelized model**,** had ranges of 0.664 to 1.040 mGy/mAs and 0.604 to 0.957, respectively. $D_{bone,2}$ and $D_{bone,3}$ had coefficients of variation of less than 27% and 29% within each tally region, respectively, and had differences of less than 13% across all models. Using a paired t-test, $D_{bone,2}$ and $D_{bone,3}$ were found to be statistically different from each other ($t=7.95$, $P < 0.0001$). The results for $D_{bone,2}$ and $D_{bone,3}$ are summarized in **Table VI**.

Table VI: Mean bone doses by tally region type with coefficients of variation within each tally region and percent difference between the means of each region

Name	Slab (2)		Entire scan volume (3)		
	$D_{bone,2}$ (mGy/mAs)	CV	$D_{bone,3}$ (mGy/mAs)	CV	%Difference
Peds1	0.917	27%	0.894	29%	2.5%
Baby	1.040	6%	0.957	14%	8.6%
Peds2	0.929	8%	0.916	11%	1.4%
Peds3	0.839	16%	0.768	21%	9.2%
Peds4	0.759	18%	0.731	24%	3.9%
Irene	0.730	9%	0.697	12%	4.8%
Peds5	0.857	14%	0.768	19%	12%
Child	0.792	5%	0.733	15%	8.1%
Helga	0.734	10%	0.651	16%	13%
Golem	0.723	8%	0.688	15%	5.2%
Donna	0.750	9%	0.680	13%	10%
Frank	0.664	10%	0.604	17%	10%
Visible Human	0.673	13%	0.603	18%	12%
Regina	0.730	9%	0.693	11%	5.4%
Rex	0.661	8%	0.636	11%	3.9%

3.A.3 Mass-weighted average

$D_{wt\text{-}avg,2}$ and $D_{wt\text{-}avg,3}$, for each voxelized model**,** had ranges of 0.306 to 0.397 mGy/mAs and 0.380 to 0.472, respectively. $D_{wt\text{-}avg,2}$ and $D_{wt\text{-}avg,3}$ had a difference of less than 24% across all patient models with $D_{wt\text{-}avg,3}$ consistently having the larger value across all patient models and all sizes. These differences were statistically different using a paired t-test ($t=15.89$, $P < 0.0001$). The results for $D_{wt\text{-}avg,2}$ and $D_{wt\text{-}avg,3}$ are shown in **Table VII**.

Table VII: $D_{wt\text{-}avg,2}$, $D_{wt\text{-}avg,3}$, and percent difference between the means

Name	Slab (2) $D_{wt\text{-}avg,2}$ (mGy/mAs)	Entire scan volume (3) $D_{wt\text{-}avg,3}$ (mGy/mAs)	% Difference
Peds1	0.366	0.436	-16%
Baby	0.397	0.472	-16%
Peds2	0.338	0.412	-18%
Peds3	0.359	0.399	-10%
Peds4	0.326	0.395	-17%
Irene	0.328	0.417	-21%
Peds5	0.326	0.408	-20%
Child	0.324	0.397	-18%
Helga	0.311	0.398	-22%
Golem	0.351	0.411	-15%
Donna	0.350	0.427	-18%
Frank	0.361	0.401	-10%
Vishum	0.332	0.380	-13%
Regina	0.306	0.402	-24%
Rex	0.317	0.379	-16%

3.B Size-specific, scanner-independent dose estimates

3.B.1 Normalized brain parenchyma doses and comparison with AAPM Report 204 values

Figure 4 shows normalized $D_{brain,1}$, $D_{brain,2}$, and $D_{brain,3}$ parameterized as functions of Dw, along with AAPM Report 204 conversion coefficients for the 16-cm pediatric body phantom. The coefficients of determination for normalized $D_{brain,1}$, $D_{brain,2}$, and $D_{brain,3}$ were 0.86, 0.84, and 0.88, respectively. Results from the regression analysis are summarized in **Table VIII**. ANOVA analysis showed there was no statistically significant difference between the means $D_{brain,1}$, $D_{brain,2}$, $D_{brain,3}$, and AAPM Report 204 conversion factors based on 16 cm $CTDI_{vol}$ [$F(3, 56) = 0.70$, $P = 0.56$]. The differences between $D_{brain,1}$, $D_{brain,2}$, and $D_{brain,3}$ estimates using results from the regression analysis and AAPM report 204 conversion factors were less than 5.7%, 8.4%, and 8.6%, respectively. It should be noted that the estimates based on AAPM Report 204 were consistently higher than those resulting from our Monte Carlo simulations, though by less than 10%.

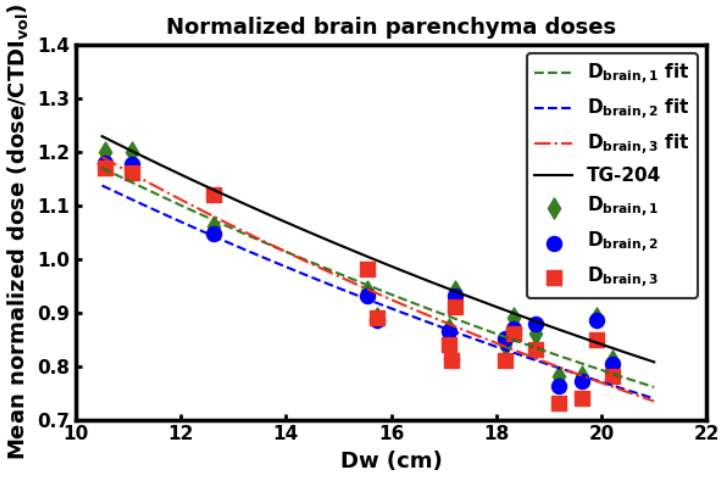

Figure 4: Normalized $D_{brain,1}$, $D_{brain,2}$, and $D_{brain,3}$ with associated regression fits. AAPM Report 204 conversion factors based 16 cm $CTDI_{vol}$ is also plotted for comparison.

Table VIII: Regression analysis results for $D_{brain,1}$, $D_{brain,2}$, and $D_{brain,3}$, and with AAPM Report 204 regression curve coefficients

Normalized dose	*A*	*B*	R^2
$D_{brain,1}$	1.80	0.041	0.86
$D_{brain,2}$	1.74	0.041	0.84
$D_{brain,3}$	1.93	0.046	0.88
AAPM Report 204	1.87	0.039	-

3.B.2 Normalized bone doses

Figure 5 contains normalized $D_{bone,2}$ and $D_{bone,3}$ parameterized as functions of Dw. The coefficients of determination for normalized $D_{bone,2}$ and $D_{bone,3}$ were 0.83 and 0.87, respectively. Results of the regression analysis are tabulated in **Table IX**.

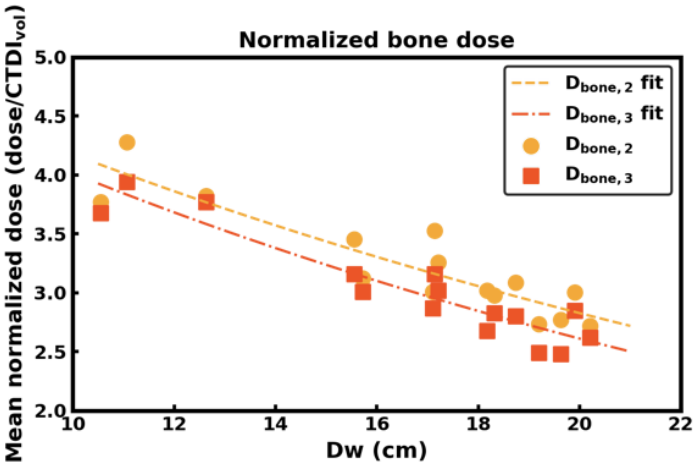

Figure 5: Normalized $D_{bone,2}$ and $D_{bone,3}$ with associated regression fits.

Table IX: Regression analysis for normalized $D_{bone,2}$ and $D_{bone,3}$

Normalized Dose	*A*	*B*	R^2
$D_{bone,2}$	6.17	0.039	0.83
$D_{bone,3}$	6.17	0.043	0.88

3.B.3 Normalized weighted average doses and comparisons to AAPM Report 204 values

Figure 6 shows normalized $D_{wt\text{-}avg,2}$ and $D_{wt\text{-}avg,3}$ parameterized as functions of Dw. The coefficients of determination for normalized $D_{wt\text{-}avg,2}$ and $D_{wt\text{-}avg,3}$ were 0.39 and 0.51, respectively. An ANOVA analysis between AAPM Report 204 conversion factors and normalized $D_{wt\text{-}avg,2}$ and $D_{wt\text{-}avg,3}$ showed a statistically significant difference [$F(2,42) = 168.1$, $P < 0.0001$]. Results from the regression analysis are summarized in **Table X**. It should be noted here that the AAPM Report 204 values are consistently lower than the $D_{wt\text{-}avg,2}$ and $D_{wt\text{-}avg,3}$ values shown in Figure 6.

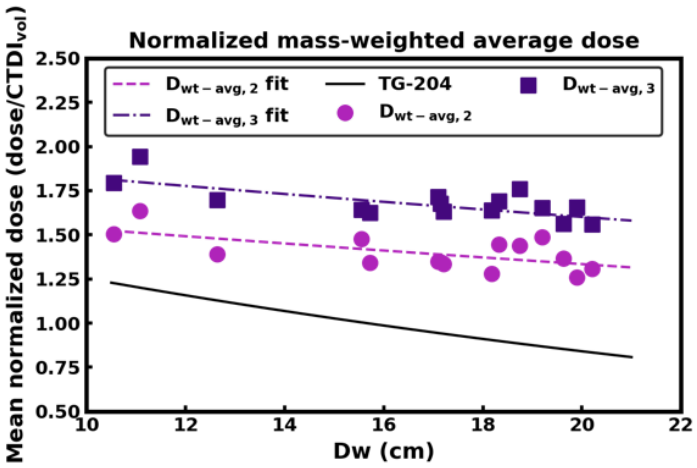

Figure 6: Normalized $D_{wt\text{-}avg,2}$ and $D_{wt\text{-}avg,3}$ with associated regression fits. AAPM Report 204 conversion factors based 16 cm $CTDI_{vol}$ is also plotted for the sake of comparison.

Table X: Regression analysis for normalized $D_{wt\text{-}avg,2}$ and $D_{at\text{-}avg,3}$

Normalized Dose	*A*	*B*	R^2
$D_{wt\text{-}avg,2}$	1.76	0.014	0.39
$D_{at\text{-}avg,3}$	2.08	0.013	0.51

4. DISCUSSION

In this study, Monte Carlo simulation methods were performed to obtain estimates of brain and bone dose from patients of different sizes and different tally configurations that could be used as a basis for determining SSDE conversion coefficients for routine, helical head examinations. Two different tally configurations were considered as possible candidates for the condition that measure dose be in the "center scan volume" as described by AAPM Report 204[6], in addition to tallying the entire scan volume of each patient. A mass-weighted average dose quantity was used to take the presence of cortical bone into consideration for the central slab configuration, as well for the entirety of the scan volume. Lastly, normalized brain parenchyma doses under all the three tally configurations and normalized mass-weighted average dose quantity for the both slab and the entire scan volume were compared with conversion coefficients from AAPM Report 204 for 16 cm pediatric body phantom.

Normalized $D_{brain,1}$, $D_{brain,2}$, and $D_{brain,3}$ had R^2 of 0.86, 0.84 and 0.88, respectively, indicated that *Dw* provides good correlative function for the normalized brain parenchyma doses under the configurations investigated in this study, including the for the entirety of the scan volume, as was also shown in McMillan et al.[8] Unlike the study conducted by McMillan et al., which only investigated normalized organ doses,[8] the current study employed meshed tallies to map dose distributions on a per voxel basis. Using this approach, $D_{brain,1}$, $D_{brain,2}$, and $D_{brain,3}$ were found to be homogeneous with CVs below 10% across all voxelized models and below 4% across all tally regions within each voxelized model. $D_{brain,1}$, $D_{brain,2}$, and $D_{brain,3}$ estimates from regression fits and AAPM Report 204 conversion factors had differences below 10% for all three configurations. Additionally, normalized $D_{brain,1}$, $D_{brain,2}$, and $D_{brain,3}$ were not significantly different than AAPM Report 204 conversion factors for 16 cm CTDI ($P = 0.56$). The implication of this result is that if "center of the scan volume" is defined as a small, central volume or a central slab within the brain parenchyma, then normalized doses within this region, as well as whole brain dose, could be reasonably estimated using the SSDE conversion coefficients from the 16 cm phantom values from AAPM Report 204. The differences observed between AAPM Report 204 and normalized $D_{brain,1}$, $D_{brain,2}$, and $D_{brain,3}$ can be attributed to the fact that the AAPM Report 204 conversion factors were originally devised to estimate dose

to the center of the scan volume for the abdomen, which is homogenous region comprised of soft tissue. The head, in contrast, is comprised of the soft-tissue brain parenchyma encased in cortical bone. The presence of the cortical bone provides an inherent source of shielding for the brain parenchyma, which decreases the normalized dose of the brain parenchyma relative to the normalized dose to the center of the scan volume for the abdomen.

$D_{bone,2}$ and $D_{bone,3}$ doses had coefficient of variation of upwards of 29% and 27%, respectively. Variations of surface dose as high as 30% for helical scans were previously observed by the Zhang et al. as a consequence of wider beam collimations and tube start angle.[22] When investigating the surface dose profile of a 32 cm CTDI phantom using MC, for example, Zhang et al. noted substantial dose peaks when utilizing a pitch of less than one and when the simulated beam width were wider than the nominal beam width.[22] A similar effect was seen when investigating the variability of surface dose in anthropomorphic phantoms in the abdominal and thoracic regions whereby, a pitch 0.75 resulted in a 37% increase in surface was shown.[22] The results of this study indicate that the variations observed within dose voxels of the cortical bone could be due to surface dose variations, particularly given the use of the low pitch and wide beam collimations recommended in the AAPM's Adult Routine Head CT Protocol.[15]

The coefficients of determination for normalized $D_{bone,2}$ and $D_{bone,3}$ were 0.83 and 0.87, respectively, indicating, as with normalized $D_{brain,1}$, $D_{brain,2}$, and $D_{brain,3}$, Dw provides good correlative function for normalized cortical bone dose either for the entirety of the head or for a central slab. The motivation for investigating dose to cortical bone as a function of patient size comes from the fact that, within the cranium, there is a fair amount of active red bone marrow (RBM), particularly in pediatric patients, with the active marrow percentage being 12% for children 10 years age and up to 29%-27% for infant patients.[23, 24] The cranium is composed of the inner and outer layers of cortical bone that enclose bone spongiosa, wherein RBM, yellow bone marrow (YBM), and trabecular bone are found.[24] Active RBM is the primary tissue of interest for the radiogenic risk of leukemia and is considered highly radiosensitive, as reflected by the tissue weighting designation in ICRP 103 ($w_T = 0.12$).[25] In this study, RBM and YBM were not modeled. The cranial microdosimetry necessary to accurately assess dose RBM is beyond the scope of this study, as is

assessing the leukemia risk associated with head CT procedures, since SSDE was only intended to estimate patient dose using metrics of radiation output displayed by scanners and was not intended to asses cancer risk from CT procedures.[6] In routine head exams, such as those recommended in AAPM's Adult Routine Head CT Protocol,[15] though the cortical bone would provide some shielding for the spongiosa containing RBM, RBM within the cranium could nevertheless be irradiated. The potential effects of RBM dose should be taken into consideration as a consequence of the scanning techniques used in routine head exams, particularly for pediatric patients.[25, 26]

In accordance with the second interpretation of "center of scan volume," this study also investigated dose to a central slab of head, which consists of both cortical bone and brain parenchyma. A mass weighted-average of the dose contributions of both cortical bone and brain parenchyma was devised to take into consideration the presence of both tissue types. The coefficients of determination for normalized $D_{wt\text{-}avg,2}$ and $D_{wt\text{-}avg,3}$ were 0.39 and 0.51, respectively. The loss of exponential relationship effects with respect to the normalized mass-weighted average dose and patient size can be explained by considering relationship between bone mass (and tissue mass) fraction of the head as a function of patient size. The mass of cortical bone increases with age which competes with the decreasing exponential of normalized dose versus patient size. Weighting normalized doses of brain parenchyma and cortical bone by their respective masses accounts for the effects of size of the patients in effect, making the relationship of normalized weighted average dose more linear with respect to patient size.

In summary, the aim of this study was to develop conversion coefficients for routine helical head CT procedures using MC methods and voxelized patient models for two interpretations of "center of the scan volume" that may be used in a manner similar to those described in in AAPM Report 204.[6] ANOVA analysis employed herein comparing AAPM Report 204 conversion factors based on 16 cm CTDI phantom with normalized brain parenchyma dose to a central point, a central slab, or the entire scan volume, revealed that the conversion factors found in AAPM Report 204 can be used as a basis for head SSDE only if dose to the brain parenchyma is considered. On the other hand, the conversion coefficients in AAPM Report 204 are not applicable when the definition of center of the scan volume includes dose to cortical bone. A

different metric, such as mass-weighted average dose, is needed to assess the dose contributions of both tissue types.

REFERENCES

[1] F.A. Mettler *et al.*, "Radiologic and Nuclear Medicine Studies in the United States and Worldwide: Frequency, Radiation Dose, and Comparison with Other Radiation Sources—1950–2007," Radiology **253**(2), 520–531 (2009).

[2] R. Smith-bindman *et al.*, "Radiation Doses in Consecutive CT Examinations from Five University of California Medical Centers," Radiology **0**(0), 1–8 (2015).

[3] C.H. McCollough, "CT dose: how to measure, how to reduce.," Health Phys. **95**(5), 508–17 (2008).

[4] M.F. McNitt-Gray, "AAPM/RSNA Physics Tutorial for Residents: Topics in CT Radiation Dose in CT1," Radiographics **22**(6), 1541–1553 (2002).

[5] A.C. Turner *et al.*, "The feasibility of patient size-corrected, scanner-independent organ dose estimates for abdominal CT exams.," Med. Phys. **38**(2), 820–9 (2011).

[6] AAPM Report 204, *Size-Specific Dose Estimates (SSDE) in Pediatric and Adult Body CT Examinations* (College Park, MD, 2011).

[7] B.M. Moore, S.L. Brady, A.E. Mirro, and R.A. Kaufman, "Size-specific dose estimate (SSDE) provides a simple method to calculate organ dose for pediatric CT examinations," Med. Phys. **41**(7), 1–10 (2014).

[8] K. McMillan, M. Bostani, C. Cagnon, M. Zankl, A.R. Sepahdari, and M. McNitt-Gray, "Size-specific, scanner-independent organ dose estimates in contiguous axial and helical head CT examinations," Med. Phys. **41**(12), 121909 (2014).

[9] AAPM Task Group 220, *Use of Water Equivalent Diameter for Calculating Patient Size and Size-Specific Dose Estimates (SSDE) in CT* (College Park, MD, 2014).

[10] N. Petoussi-Henss, M. Zankl, U. Fill, D. Regulla, and M. Zanki, "The GSF family of voxel

phantoms," Phys. Med. Biol. **47**(1), 89–106 (2002).

[11] International Commission on Radiological Protection, "Adult reference computational phantoms," ICRP Publ. 110. Ann. ICRP 39 **(2)**, (2009).

[12] M. Zankl, K.F. Eckerman, and W.E. Bolch, "Voxel-based models representing the male and female ICRP reference adult - The skeleton," Radiat. Prot. Dosimetry **127**(1–4), 174–186 (2007).

[13] ICRU, "ICRU Report 44, Tissue Substitutes in Radiation Dosimetry and Measurement," J. Int. Comm. Radiat. Units Meas. (1993).

[14] J.J. Demarco, T.D. Solberg, and J.B. Smathers, "A CT-based Monte Carlo simulation tool for dosimetry planning and analysis," Med. Phys. **25**, 1–11 (1998).

[15] American Association of Physicists in Medicine, *Adult Routine Head CT Protocols Version 2.0*, 1–20 (2016).

[16] D.B. Pelowitz, "MCNPX User's Manual," in *MCNPX User's Man.*(Los Alamos, NM, 2011).

[17] AAPM Task Group 195, *Monte Carlo Reference Data Sets for Imaging Research* (College Park, MD, 2015).

[18] M. Bostani *et al.*, "Accuracy of Monte Carlo simulations compared to in-vivo MDCT dosimetry.," Med. Phys. **42**(2), 1080 (2015).

[19] M.B. Chadwick *et al.*, "ENDF/B-VII.1 nuclear data for science and technology: Cross sections, covariances, fission product yields and decay data," Nucl. Data Sheets **112**(12), 2887–2996 (2011).

[20] J.J. DeMarco *et al.*, "A Monte Carlo based method to estimate radiation dose from multidetector CT (MDCT): cylindrical and anthropomorphic phantoms.," Phys. Med. Biol. **50**(17), 3989–4004 (2005).

[21] A.C. Turner *et al.*, "A method to generate equivalent energy spectra and filtration models based on measurement for multidetector CT Monte Carlo dosimetry simulations.," Med. Phys. **36**(6), 2154–2164 (2009).

[22] D. Zhang *et al.*, "Variability of surface and center position radiation dose in MDCT: Monte Carlo

simulations using CTDI and anthropomorphic phantoms.," Med. Phys. **36**(3), 1025–38 (2009).

[23] ICRP 70, "Basic Anatomical & Physiological Data for use in Radiological Protection - The Skeleton," Ann. ICRP (2), (1995).

[24] M. Cristy, "Active bone marrow distribution as a function of age in humans.," Phys. Med. Biol. **26**, 389–400 (1981).

[25] ICRP, "The 2007 Recommendations of the International Commission on Radiological Protection," ICRP Publ. 103. Ann. ICRP 37 (2007).

[26] M.S. Pearce *et al.*, "Radiation exposure from CT scans in childhood and subsequent risk of leukaemia and brain tumours: A retrospective cohort study," Lancet **380**(9840), 499–505 (2012).